Electronic Research Archive

http://www.aimspress.com/journal/era

ERA, 31(10): 6120–6133.
DOI: 10.3934/era.2023311
Received: 03 April 2023
Revised: 22 August 2023
Accepted: 27 August 2023
Published: 13 September 2023

Research article

Characteristic period analysis of the Chinese stock market using successive one-sided HP filter

Yuxia Liu[1], Qi Zhang[2,*], Wei Xiao[1] and Tianguang Chu[1]

[1] College of Engineering, Peking University, Beijing 100871, China
[2] School of Information Technology and Management, University of International Business and Economics, Beijing 100029, China

* **Correspondence:** Email: zhangqi@uibe.edu.cn.

Abstract: Time series of stock indices usually exhibit nonstationary and chaotic behavior. Analysis of the characteristics of the business cycle can reveal pertinent insights into the evolution of the stock volatility. This paper studies the characteristic periods of three main Chinese stock indices, i.e., the Shanghai composite index (SHCI), the Shenzhen component index (SZCI), and the Hang Seng index (HSI). We propose an approach based on the successive one-sided Hodrick-Prescott (SOHP) filtering and wavelet analysis of the empirical data from the stock markets, to detect their characteristic periods. In particular, the SOHP filter, which preprocesses the time series with a moving-horizon optimization procedure, enables us to extract the volatility cycles in different time scales from a stock time series and reduce noise distortion. The characteristic period of the stock index is then determined by the maxima of the wavelet power spectrum of the filtered data. The evolution of the characteristic period in time demonstrates rich information concerning the period stability of the stock market, as well as the cause and effect of the stock crash. To facilitate solving the moving-horizon optimization issue of the SOHP filter, we also present an incremental HP filtering algorithm, which greatly simplifies the involved inverse matrix operation in the HP-type filters.

Keywords: nonlinear time series; characteristic period; the successive one-sided HP filter; incremental HP filtering algorithm; Chinese stock market

1. Introduction

Stock markets have long been studied as complex systems with the time series of stock prices as observation variables of the underlying dynamics [1–4]. A basic issue addressed in the studies concerns characterizing the cyclicality of stock fluctuations [5, 6]. Generically, the volatility of stock markets demonstrates complicated dynamic features, with nonstationary evolution component and many coexisting modes of oscillations simultaneously. Corresponding to this, the time series arising from stock markets include long-term growth trend as well as short-term fluctuations. In the context of macroeconomics, the business cycles of the stock markets are characterized by their short-term fluctuations [7]. Researching the major cyclical behavior can provide insight into the stock market movement and help in making decisions on the stock market [8].

In the literature, several methods have been proposed to separate the trend from the cyclical component in stock time series [9, 10]. A most popular approach is that based on the Hodrick-Prescott (HP) filter and its variants [11–13]. The basic idea of the HP filter is to split a time series into its trend (or secular) and cyclical component, and separate them by minimizing the variance of cyclical variable subject to a penalty for variation in the second difference of trend variable. It was originally proposed for study of the postwar U.S. business cycles [11] and later widely employed in econometrics [14], due to its simplicity in formulation and less assumption on data statistics. Observe that the HP filter itself is a two-sided filter, namely, it processes both future and past data in batch to determine the trend component. This may result in a smooth fitting of the trend and distort the extracted cyclical components. To address this issue, Refs. [12] and [15] suggested a one-sided HP filter (OHP) that applies the HP filter on an expanding sample so as to filtering out less fluctuations at each time point.

The aim of this paper is to further develop a successive one-sided HP filter (SOHP) from the perspective of multi-time scale decomposition, with application to characteristic period analysis of the Chinese stock market. To motivate our study, we regard the primary HP filter as an operation to split the time series into slow- and fast-varying variables, corresponding to the trend and the cyclical component respectively. Hence, applying the operation recursively on the updated fast-varying variable will enable us to extract the cycles of stock volatility on different time scales. This finally yields a successive expansion of the original time series in different time scales, as an adaptation form for time-frequency analysis after removing the trend from it. In this way, we will evaluate the characteristic periods of the main Chinese stock indices, i.e., the Shanghai composite index (SHCI), the Shenzhen component index (SZCI), and the Hang Seng index (HSI) [16], by determining the maxima of the wavelet power spectrum of the filtered data; and examine the evolution of the characteristic periods along with their implications. In particular, our results reveal the period stability and suggest possible relation between period shift and stock crash.

We note that the proposed SOHP filter is essentially an optimization problem with moving horizon. Solving the problem involves the inverse operation of a matrix with ever increasing size. The existing OHP filtering algorithm is originally designed for the case of fixed-length data and is hence inconvenient for the SOHP filter. To overcome this difficulty, we also present an incremental HP filtering algorithm, which can compute the required inverse matrices for growing-length data in a recursive manner, greatly facilitating the operation of HP-type filters in modern data-rich environments.

The rest of this paper is organized as follows. In Section 2, we introduce the SOHP filter and the new filtering algorithm. Section 3 presents analysis of the chaotic features and the characteristic periods of the concerned Chinese stock indices. A summary is drawn in Section 4.

2. The SOHP filter and incremental filtering algorithm

This section introduces the proposed SOHP filter and presents an incremental filtering algorithm.

2.1. The SOHP filter

We first recall the HP filter [11], which decomposes l observations of a variable y_t into the following form:

$$y_t = g_t + c_t, \quad t = 1, 2, \dots, l, \tag{2.1}$$

where g_t represents the growth trend and c_t the cyclical volatility, corresponding to the low- and high-frequency components of y_t, respectively. The trend g_t are determined by the minimization problem

$$\min_{g_t} \left\{ \sum_{t=1}^{l} (y_t - g_t)^2 + \eta \sum_{t=3}^{l} (g_t - 2g_{t-1} + g_{t-2})^2 \right\}, \tag{2.2}$$

where $\eta \geq 0$ is a tuning parameter. Let $\boldsymbol{y}_l = [y_1, y_2, \cdots, y_l]^\top$, $\boldsymbol{g}_l = [g_1, g_2, \cdots, g_l]^\top$, and the tridiagonal matrix

$$F_l = \begin{bmatrix} 1 & -2 & 1 & \cdots & 0 & 0 & 0 \\ \cdots & \cdots & \cdots & \cdots & \cdots & \cdots & \cdots \\ 0 & 0 & 0 & \cdots & 1 & -2 & 1 \end{bmatrix}_{(l-2)\times l},$$

one can rewrite the problem (2.2) in a compact form as

$$\min_{\boldsymbol{g}_l} \left\{ \|\boldsymbol{y}_l - \boldsymbol{g}_l\|^2 + \eta \|F_l \boldsymbol{g}_l\|^2 \right\}, \tag{2.3}$$

where $\|\cdot\|$ represents the ℓ_2-norm of a vector. The solution to the optimization problem (2.3) is given by

$$\boldsymbol{g}_l = S_l^{-1} \boldsymbol{y}_l, \tag{2.4}$$

and hence the cyclical part is

$$\boldsymbol{c}_l = (I_l - S_l^{-1}) \boldsymbol{y}_l, \tag{2.5}$$

where $S_l = I_l + \eta F_l^\top F_l$ and I_l is the $l \times l$ identity matrix.

In macroeconomic analysis the slow-varying part $\boldsymbol{g}_l$ represents a secular trend of economic growth, and the fast-varying part $\boldsymbol{c}_l$ represents the short-term fluctuation of economic volatility [11, 17]. Observe that the HP filter decomposes a stock price time series into its trend and cycle parts using both its past and future data at a given period. This can result in a smooth fitting of the growing trend of the stock price and might lose certain fluctuation details of the trend. In view of this, a modified HP filter, namely the one-sided HP filter was proposed in [12], which applies the HP filter to the presently available sample only to avoid using future data at a given time. Specifically, the one-sided HP filter performs the HP filter on an expanding sample by letting

$$Y = \begin{bmatrix} y_1 & y_1 & \cdots & y_1 \\ 0 & y_2 & \cdots & y_2 \\ \vdots & \vdots & \ddots & \vdots \\ 0 & 0 & \cdots & y_l \end{bmatrix}_{l\times l}$$

be the observation matrix formed by the y_t, with each column the ample data available at an observation time; and exerting Eq (2.4) to each column of Y to yield the HP trend matrix

$$G = \begin{bmatrix} g_{1,1} & g_{1,2} & \cdots & g_{1,l} \\ 0 & g_{2,2} & \cdots & g_{2,l} \\ \vdots & \vdots & \ddots & \vdots \\ 0 & 0 & \cdots & g_{l,l} \end{bmatrix}_{l\times l}.$$

$$\boldsymbol{g}^O = [g_{1,1}, g_{2,2}, \ldots, g_{l,l}]^\top.$$

In the present study, we will employ the one-sided HP filter in a recursive manner to reduce the data noise and extract the volatility tendencies of the time series on different frequencies or time scales. This leads to a successive expansion of the concerned time series in different time scales that admits wavelet analysis after removing the secular trend. To be specific, we apply the one-sided HP filter recursively to the fast-varying component obtained in the last step of operation, following the procedure as below:

Step 1. Apply the OHP filter to the data and obtain the trend $\boldsymbol{g}_l^{O(1)} = \boldsymbol{g}_l^O$ and the residual $\boldsymbol{c}_l^{O(1)} = \boldsymbol{y}_l - \boldsymbol{g}_l^{O(1)}$;

Step 2. Assume that for $i > 1$, the cycle residual $\boldsymbol{c}^{O(i)}$ is available, apply the OHP filter to $\boldsymbol{c}_l^{O(i)}$ to obtain higher order components $\boldsymbol{g}_l^{O(i+1)}$ and $\boldsymbol{c}_l^{O(i+1)}$, and repeat this operation on the updated cycle residual until certain stopping criterion (to be stated later) is met;

Step 3. Sum up all the trend components $\boldsymbol{g}_l^{O(1)}, \ldots, \boldsymbol{g}_l^{O(n)}$ of different scales successively obtained in n iterations in *Step 2* to get the finite expansion form of the trend estimate:

$$\overline{\boldsymbol{g}}_l = \sum_{i=1}^{n} \boldsymbol{g}_l^{O(i)}, \tag{2.6}$$

where $\boldsymbol{g}_l^{O(i)}$ denotes the i-th trend residul obtained in *Step 2*. We will refer to the above approach as the *successive one-sided HP (SOHP) filter*.

Analogous to the case of the bHP filter [13], here we introduce the following Bayesian-type information criterion (BIC) as the iteration stop condition for the SOPH in *Step 2* : Let

$$BIC(n) = \frac{\|\boldsymbol{c}^{O(n)}\|_1}{\|\boldsymbol{c}^{O(1)}\|_1} + \frac{1}{l-2}\sum_{t=3}^{l} \frac{\mathrm{tr}(M_t^{(n)})}{\mathrm{tr}(I_t - S_t^{-1})}, \tag{2.7}$$

where $\|\cdot\|_1$ represents ℓ_1-norm of a vector, $\boldsymbol{c}^{O(n)}$ denotes the n-th cyclic residual yielded thereof, $\mathrm{tr}(\cdot)$ represents the trace of a matrix, and $M_t^{(n)} = I_t - (I_t - S_t^{-1})^n$; the proper number of iterations n corresponds to the smallest BIC value.

The expansion form (2.6) can be viewed as a preprocess of a raw time series to reduce noise and extract volatility trends on different time scales. In contrast to the HP filtering, the adoption of one-sided HP filter algorithm in this stage can help to avoid smoothing out extra fluctuations in the filtered data.

In the next stage, we use the HP filter to remove the secular growth term from $\overline{\boldsymbol{g}}$ to obtain the detrended component $\tilde{\boldsymbol{c}} = [\tilde{c}_1, \tilde{c}_2, \cdots, \tilde{c}_l]^\top$, which involves periodic motions in different time scales. The characteristic period of the time series refers to the principal period component identified in wavelet analysis of the cyclical component $\tilde{\boldsymbol{c}}$, to be specified later. Notice that, as mentioned before, the HP filtering usually results in a smoother growth trend than the one-sided HP filter does because it makes use of both past and future data. Therefore, the corresponding detrended residual component by the HP filter would reserve more fluctuations of stock volatility, and is hence much relevant to the purpose of our study.

2.2. Incremental HP filtering algorithm

Notice that the OHP filter is essentially an optimization problem with moving horizon, and the Eqs (2.4) and (2.5) explicitly depend on the length l of the time series. When the length increases, one has to compute the inverse of a new matrix S_l of higher dimension. This would impede application of the formulas in expanding sample or streaming data scenario. Actually, even for a time series of fixed length it is usually not desirable to take inverse operation for a matrix of large size directly. To address this issue, we propose an incremental algorithm for the HP filter as follows. For $4 \le t \le l$, define

$$F_t = \begin{bmatrix} \tilde{F}_{t-1} \\ \boldsymbol{p}_t^\top \end{bmatrix}_{(t-2)\times t},$$

where $\tilde{F}_{t-1} = [F_{t-1} \quad \mathbf{0}]_{(t-3)\times t}$ and $\boldsymbol{p}_t = [0, \dots, 0, 1, -2, 1]^\top \in \mathbb{R}^t$, we have

$$\begin{aligned} S_t &= I_t + \eta F_t^\top F_t \\ &= \begin{bmatrix} S_{t-1} & \\ & 1 \end{bmatrix} + \eta \boldsymbol{p}_t \boldsymbol{p}_t^\top. \end{aligned}$$

By the Woodbury matrix identity [18], we get the following recursive formula

$$\begin{cases} S_t^{-1} = \begin{bmatrix} S_{t-1}^{-1} & \\ & 1 \end{bmatrix} - \left(\dfrac{1}{\eta} + \boldsymbol{p}_t^\top \boldsymbol{q}_t \right)^{-1} \boldsymbol{q}_t \boldsymbol{q}_t^\top, \\ S_3^{-1} = \dfrac{1}{6\eta + 1} \begin{bmatrix} 5\eta + 1 & 2\eta & -\eta \\ 2\eta & 2\eta + 1 & 2\eta \\ -\eta & 2\eta & 5\eta + 1 \end{bmatrix}, \end{cases} \tag{2.8}$$

where

$$\boldsymbol{q}_t = \begin{bmatrix} S_{t-1}^{-1} & \\ & 1 \end{bmatrix} \boldsymbol{p}_t, \quad \text{for } 4 \le t \le l.$$

Let $\boldsymbol{y}_t = [y_1, y_2, \cdots, y_t]^\top$, from Eqs (2.4) and (2.8), the growth trend and the cyclical component of $\boldsymbol{y}_t$ are given by

$$\begin{aligned} \boldsymbol{g}_t &= S_t^{-1} \boldsymbol{y}_t \\ &= \begin{bmatrix} \boldsymbol{g}_{t-1} \\ y_t \end{bmatrix} - \delta_t (g_{t-2} - 2g_{t-1} + y_t) \boldsymbol{q}_t, \end{aligned} \tag{2.9}$$

and

$$\begin{aligned} \boldsymbol{c}_t &= \boldsymbol{y}_t - \boldsymbol{g}_t \\ &= \begin{bmatrix} \boldsymbol{c}_{t-1} \\ 0 \end{bmatrix} + \delta_t (g_{t-2} - 2g_{t-1} + y_t)\boldsymbol{q}_t, \end{aligned} \tag{2.10}$$

respectively, where

$$\delta_t = \frac{1}{\frac{1}{\eta} + \boldsymbol{p}_t^\top \boldsymbol{q}_t}.$$

We refer to Eqs (2.8)–(2.10) as an *incremental HP filtering algorithm*, which merely requires evaluating a 3×3 initial inverse matrix and applies effectively to series data of fixed as well as expanding length in a recursive manner.

3. Characteristic period analysis of the Chinese stock market

This section presents the results on dynamic behavior analysis of the Chinese stock market. We select the monthly data of SHCI from July 1997 to September 2020, SZCI from October 1997 to September 2020, and HSI from October 1987 to September 2020. Let y_t be the log-transformation of these stock indices. Applying the method described in Section 2.1 to y_t, we can obtain the detrended residual $\tilde{\boldsymbol{c}}$ for each stock index respectively, as shown in Figure 1, where the filter parameter $\eta = 14,400$ for all cases as suggested in [19]. According to our numerical experiments, the *BIC* in Eq (2.7) assumes its minimum value at $n = 3$ for the three stock indices. Table 1 shows the mean and the variance of the final c_t, and the *BIC* value for our SOHP method. It can be seen that the mean value of c_t is very close to zero for each case. In the following, we will discuss the dynamic behavior of the stock volatility based on $\tilde{\boldsymbol{c}}$.

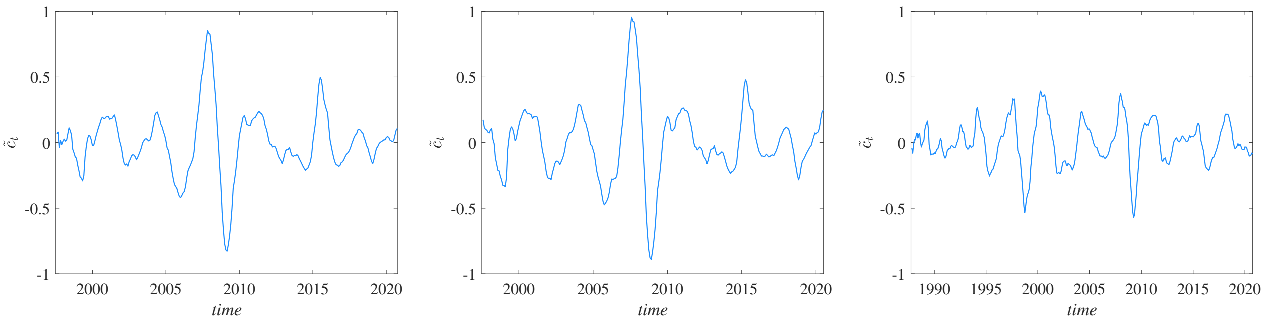

(a) (b) (c)

Figure 1. Plots of the cyclical component $\tilde{\boldsymbol{c}}$ of the stock indices, obtained from the empirical data $\boldsymbol{y}$ by preprocessing with the SOHP filter and detrending with the HP filter, for the case of (a) SHCI, (b) SZCI, and (c) HSI.

Table 1. The mean, the variance, and the *BIC* for SOHP filter with $n = 3$.

Index	Mean	Variance	*BIC*
SHCI	−5.01e-5	1.75e-2	0.9659
SZCI	−1.32e-4	2.20e-2	0.9652
HSI	5.13e-4	9.30e-3	0.9600

3.1. *Autocorrelation coefficients*

We first evaluate the autocorrelation function of $\tilde{\boldsymbol{c}}$, which measures the correlation between the data and itself at different time points, defined as

$$\rho_d = \frac{E[(\tilde{c}_t - \mu)(\tilde{c}_{t+d} - \mu)]}{\sqrt{E[(\tilde{c}_t - \mu)^2]E[(\tilde{c}_{t+d} - \mu)^2]}},$$

where $\mu = E[\tilde{\boldsymbol{c}}]$, $E[\cdot]$ denotes the average or expectation value of a variable, and d is the lag order [20, 21]. Figure 2 displays the computational results for the three stock indices. It indicates that ρ_d has a period of about three years for each case, which is within the range of the commonly recognized macroeconomic volatility cycles [22]. Also, it is clear from Figure 2 that ρ_d exhibits a decaying oscillation around and eventually tending to zero. This is regarded as a typical character of chaotic oscillations in a nonlinear dynamical system [23].

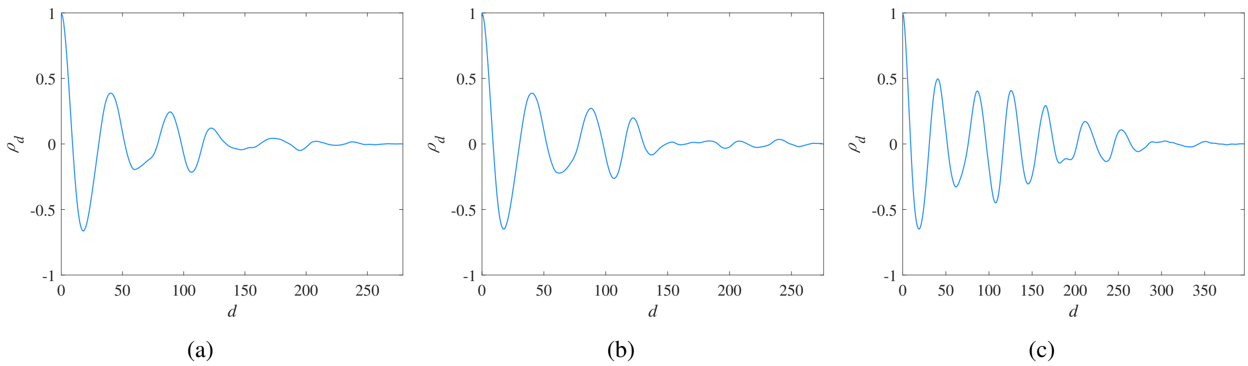

Figure 2. Plots of the autocorrelation coefficients. The period $P = 4 \times d_0$ years, d_0 is the lag order when the autocorrelation coefficient first decays to zero. (a) SHCI, $P_{SHCI} = 3.3$ years; (b) SZCI, $P_{SZCI} = 3$ years; (c) HSI, $P_{HSI} = 3.3$ years.

3.2. *Phase diagrams and fractal dimensions of the chaotic attractors*

In order to examine the chaotic behavior of the cyclical residual $\tilde{\boldsymbol{c}}$ in more detail, we employ the delay coordinate method to reconstruct a phase trajectory from the one-dimensional time series that is topologically equivalent to the underlying dynamics of the original time series. Figure 3 depicts the phase diagrams for the subseries $\tilde{\boldsymbol{c}}$ of SHCI, SZCI, and HSI with the delay time $d = 7$ and the embedded dimension of 2, where the delay time is selected according to the literature [24]. The plots exhibit spiral-shaped feature, indicating a typical chaotic behavior [23]. In addition, by using the box counting method, we also calculate the fractal dimensions of the chaotic attractors for the cases of SHCI, SZCI, and HSI as 1.11, 1.11, and 1.16, respectively [25].

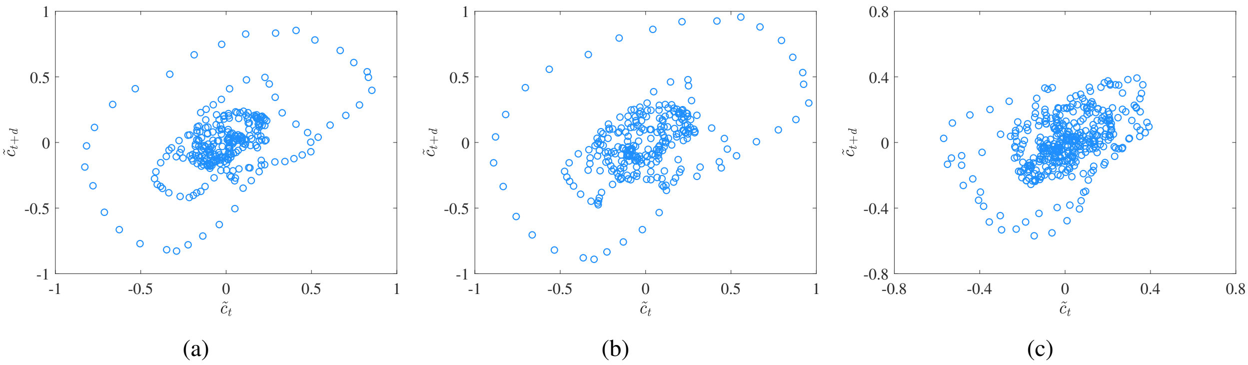

Figure 3. Phase diagrams and fractal dimensions (FD) of the chaotic attractors for the case of (a) SHCI, $FD_{SHCI} = 1.11$; (b) SZCI, $FD_{SZCI} = 1.11$; and (c) HSI, $FD_{HSI} = 1.16$.

3.3. Characteristic period of stock price volatility

The chaotic behavior as demonstrated before indicates the coexistence of oscillatory modes in the underlying dynamics of the stock time series. Next we proceed to determine the characteristic periods of them through wavelet analysis of the detrended residual $\tilde{\boldsymbol{c}}$. By characteristic period of a signal we meant the reciprocal of the frequency corresponding to the peak of the wavelet coefficient of the signal in each time cross-section [23]. The characteristic period of a stock market represents the instantaneous principal oscillatory mode, which corresponds to the period determined by the maxima of the wavelet power spectrum, effectively capturing the major variability of the stock price and portraying the multi-frequency dynamical behavior of the stock index time series. Figure 4 shows the resulting time-frequency contour maps. It can be seen that the frequency corresponding to the peak of the wavelet coefficient at different moments approximately ranges from 0.2 to 0.5. That is, the characteristic period at different times is between about 2 and 5 years.

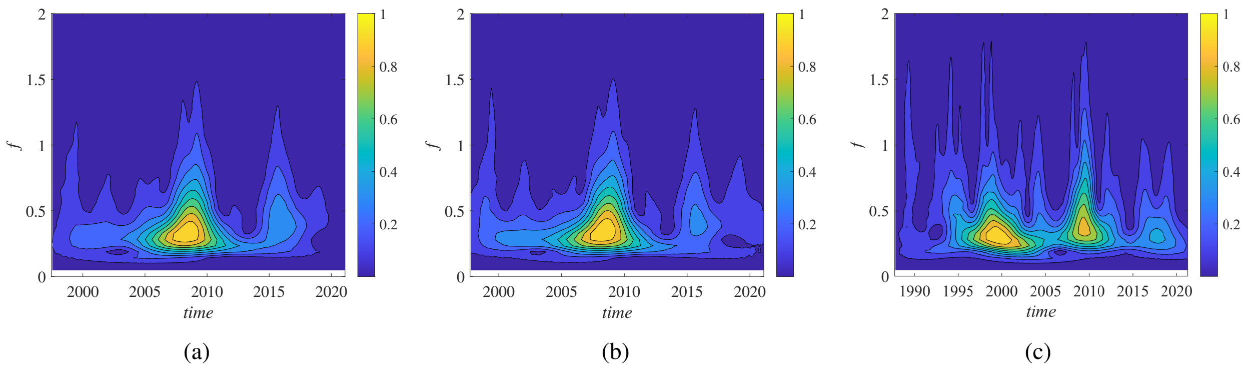

Figure 4. Time-frequency contour maps for the case of (a) SHCI, (b) SZCI, and (c) HSI.

Figure 5 illustrates the evolution of characteristic periods of SHCI, SZSI, and HSI. Roughly speaking, the characteristic period for each case can remain a constant value in about 3 to 4 years. It will shift in face of shocks and then recover to near the previous value over time. This suggests certain degree of stability of the characteristic period for the concerned Chinese stock market. To quantify the argument, we further compute the characteristic period variability, which is measured as the ratio of the standard deviation to the mean of the periods. The results for SHCI, SZCI, and HSI are 17.8% over 23 years, 18.2% over 23 years, and 21.4% over 33 years, respectively. The period stability of business cycles in the stock markets are remarkable. By comparison, the characteristic period variability of the HSI is slightly larger than that of the SHCI and SZCI, implying a relatively less period stability and more volatility of the former.

We can learn more from the characteristic period shifts of the stock markets as shown in Figure 5. In particular, an abrupt downward shift in the characteristic period curve indicates a rapid change from low to high frequency of the variation in stock price, meaning that the stock market becomes very active in a short time interval. This can often be regarded as a precursor to the stock market crash. From Figure 5, the SHCI has 3 times of downward shifts in 23 years, the SZCI has 3 times in 23 years, and the HSI has 7 times in 33 years. Table 2 lists the occurrence time of such period shift in each inset of Figure 5 along with the fall time of each stock index.

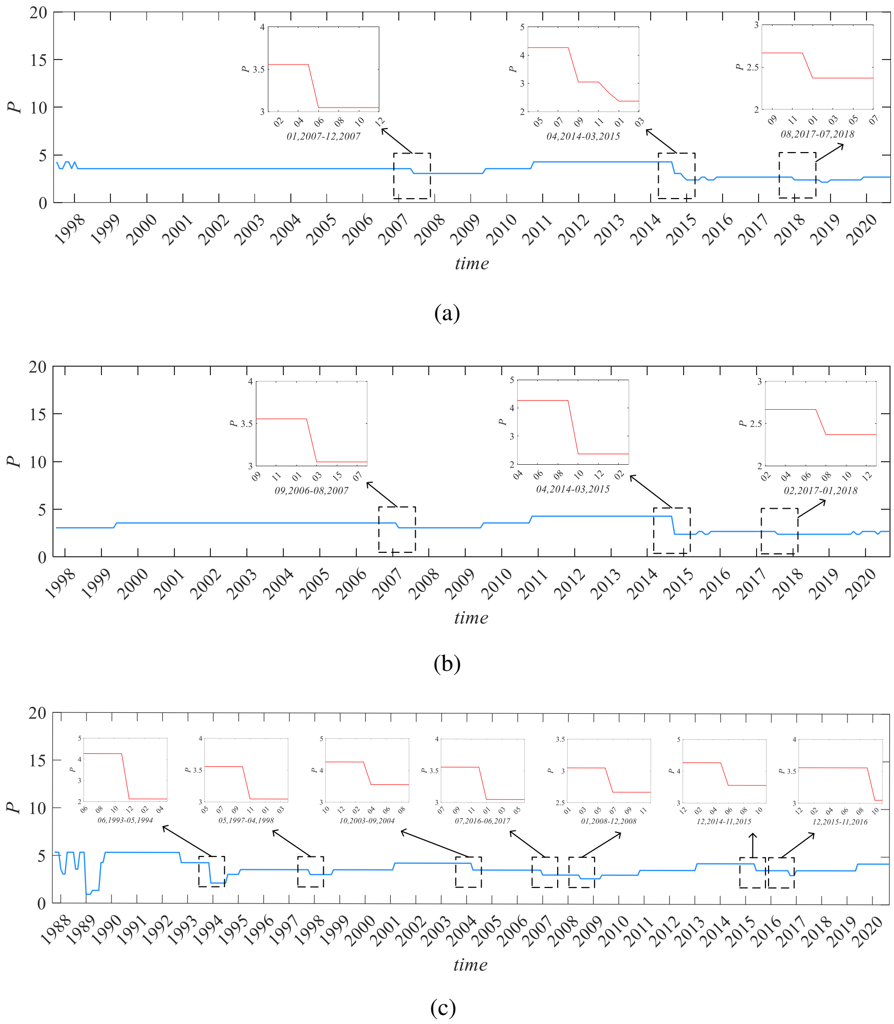

Figure 5. Characteristic periods and shifts. (a) SHCI, (b) SZCI, (c) HSI.

Table 2. Characteristic period shift time and index fall time.

Shift numbers	Period shift time	Index fall time
SHCI		
First	06.2007	10.2007 [26]
Second	09.2014	06.2015 [27]
Third	01.2018	01.2018 [16]
SZCI		
First	03.2007	10.2007 [26]
Second	10.2014	06.2015 [27]
Third	08.2017	10.2017 [16]
HSI		
First	12.1993	01.1994 [28]
Second	11.1997	08.1997 [29]
Third	04.2004	03.2004 [30]
Fourth	01.2007	10.2007 [30]
Fifth	07.2008	09.2008 [31]
Sixth	06.2015	06.2015 [32]
Seventh	10.2016	01.2018 [16]

It is of interest to note that the data in Table 2 can be categorized into two types. In the yellow area, the characteristic period shift occurs preceded or concurrent with the fall of the stock index, and the gray area represents the case otherwise. The two opposite cases indicate different routes to stock crash. In the former case a lot of short-term trading activity surges in a short time within the stock market, leading to rapid accumulation of economic bubbles, and eventually resulting in the slump in stock price. For example, in Figure 5(a), the crashes of the SHCI that occurred in October 2007 and June 2015 were caused by internal factors; the characteristic period shifted in June 2007 and September 2014 before the stock index crashed. The other cases of stock index sharp declines in the yellow area of Table 2 (corresponding to the partial enlargement in Figure 5) were also mainly due to internal factors, with shifts of the characteristic period occurring before or at the same time as stock market crashes. Whereas for the latter case the delayed characteristic period shift can be regarded as the aftermath of stock crash. According to relevant information, the second and third large fluctuations of HSI (gray data in Table 2) that occurred prior to the characteristic period shift have their own external origins. The one of price crash bursting in August 1997 is now acknowledged as a result of the Asian financial crisis that began in Thailand [33], while the other one in March 2004 is attributed to a series of global minor crash [34]. In other words, these two instances of stock market crash that occurred before the characteristic period shift are caused externally. Accordingly, one may refer to the otherwise case where the stock market crash occurs subsequent to the characteristic period shift is induced internally. As a consequence, a decline in the stock characteristic period curve may be view as an alarm of the crash for the latter case.

4. Conclusions

The fluctuations in stock markets usually demonstrate lots of coexisting oscillatory modes simultaneously. Capturing the major cyclical behavior sheds light on our better understanding of the stock market volatility and helps in planning effective investment strategies. In general, the time series from stock markets include both secular growth trend and short-term cyclical tendencies, and the business cycles of stock markets can be examined with the detrended series data.

In this paper, we have developed an approach to study the cyclical behavior of stock price volatility based on extended HP filtering and time-frequency analysis. The proposed SOHP filter together with the incremental filtering algorithm enables extraction of the volatility tendencies with different time scales in a stock time series for further investigation of the underlying dynamics. The characteristic period of a stock market represents the instantaneous principal oscillatory mode in wavelet transform of the stock time series, capturing the major variability of the stock price. Empirical results of the present approach on the three main Chinese stock market indices reveal that most of the variability of the stock prices occurs at frequencies of periods about 3 to 4 years. This agrees with the common observation of the Chinese stock market. Interestingly, our results also identify the downward shift of the characteristic period values, which are all associated with certain recorded financial crisis. According to whether the period shift occurs behind the crisis or not, the cause of change in stock volatility cycles may be regarded as external or internal. In our study, most cases (11 out of 13 instances) are internal, where short-term volatility in stock prices emerges severely and accumulates quickly, lowing the cyclical periods of the price fluctuation until the crash. This suggests that for a steadily evolving characteristic period curve of a stock index, the appearance of an evident decline in characteristic period values may be viewed as a warning of forthcoming large fluctuations.

Use of AI tools declaration

The authors declare they have not used Artificial Intelligence (AI) tools in the creation of this article.

Acknowledgments

This paper is supported by the National Natural Science Foundation of China (Grant Nos. 61673027 and 62106047), Humanity and Social Science Youth foundation of Ministry of Education, Scientific Research Laboratory of AI Technology and Applications, and University of International Business and Economics.

Conflict of interest

The authors declare there is no conflicts of interest.

References

1. N. Salmon, I. SenGupta, Fractional Barndorff-Nielsen and Shephard model: applications in variance and volatility swaps, and hedging, *Ann. Finance*, **17** (2021), 529–558. https://doi.org/10.1007/s10436-021-00394-4

2. M. Lin, I. SenGupta, Analysis of optimal portfolio on finite and small-time horizons for a stochastic volatility market model, *SIAM J. Financ. Math.*, **12** (2021), 1596–1624. https://doi.org/10.1137/21M1412281
3. T. Mo, C. Xie, K. Li, Y. Ouyang, Z. Zeng, Transmission effect of extreme risks in China's financial sectors at major emergencies: empirical study based on the GPD-CAViaR and TVP-SV-VAR approach, *Electron. Res. Arch.*, **30** (2022), 4657–4673. https://doi.org/10.3934/era.2022236
4. X. Hui, B. Sun, I. SenGupta, Y. Zhou, H. Jiang, Stochastic volatility modeling of high-frequency CSI 300 index and dynamic jump prediction driven by machine learning, *Electron. Res. Arch.*, **31** (2023), 1365–1386. https://doi.org/10.3934/era.2023070
5. N. T. Vu, Stock market volatility and international business cycle dynamics: evidence from OECD economies, *J. Int. Money Finance*, **50** (2015), 1–15. https://doi.org/10.1016/j.jimonfin.2014.08.003
6. F. Verona, Time–frequency characterization of the U.S. financial cycle, *Econ. Lett.*, **144** (2016), 75–79. https://doi.org/10.1016/j.econlet.2016.04.024
7. P. A. Samuelson, W. D. Nordhaus, *Macroeconomics*, 18^{th} edition, Posts & Telecom Press: McGraw-Hill Education (Asia) Co, 2007.
8. T. Choudhry, F. I. Papadimitriou, S. Shabi, Stock market volatility and business cycle: evidence from linear and nonlinear causality tests, *J. Banking Finance*, **66** (2016), 89–101. https://doi.org/10.1016/j.jbankfin.2016.02.005
9. R. Bisoi, P. K. Dash, A hybrid evolutionary dynamic neural network for stock market trend analysis and prediction using unscented Kalman filter, *Appl. Soft Comput.*, **19** (2014), 41–56. https://doi.org/10.1016/j.asoc.2014.01.039
10. X. L. Li, J. Yan, X. Wei, Dynamic connectedness among monetary policy cycle, financial cycle and business cycle in China, *Econ. Anal. Policy*, **69** (2021), 640–652. https://doi.org/10.1016/j.eap.2021.01.014
11. R. J. Hodrick, E. C. Prescott, Postwar US business cycles: an empirical investigation, *J. Money Credit Banking*, **29** (1997), 1–16. https://doi.org/10.2307/2953682
12. J. H. Stock, M. W. Watson, Forecasting inflation, *J. Monetary Econ.*, **44** (1999), 293–335. https://doi.org/10.1016/S0304-3932(99)00027-6
13. P. C. B. Phillips, Z. Shi, Boosting: why you can use the HP filter, *Int. Econ. Rev.*, **62** (2021), 521–570. https://doi.org/10.1111/iere.12495
14. P. Krusell, T. Mukoyama, A. Şahin, Labour-market matching with precautionary savings and aggregate fluctuations, *Rev. Econ. Stud.*, **77** (2010), 1477–1507. https://doi.org/10.1111/j.1467-937X.2010.00700.x
15. K. R. Gerdrup, A. B. Kvinlog, E. Schaanning, *Key Indicators for a Countercyclical Capital Buffer in Norway - Trends and Uncertainty*, 2013. Available from: http://hdl.handle.net/10419/210284.
16. Yahoo Finance, Stock data, *[EB/OL]*, 2020. Available from: https://hk.finance.yahoo.com/.
17. E. Kočenda, A. Černý, *Elements of Time Series Econometrics: An Applied Approach*, Charles University in Prague, Karolinum Press, 2015.

18. M. Fornasier, H. Rauhut, R. Ward, Low-rank matrix recovery via iteratively reweighted least squares minimization, *SIAM J. Optim.*, **21** (2011), 1614–1640. https://doi.org/10.1137/100811404

19. M. I. Stolbov, M. A. Shchepeleva, A. M. Karminsky, A global perspective on macroprudential policy interaction with systemic risk, real economic activity, and monetary intervention, *Financ. Innovation*, **7** (2021), 41. https://doi.org/10.1186/s40854-021-00257-x

20. H. Kantz, T. Schreiber, *Nonlinear Time Series Analysis*, 2^{nd} edition, Cambridge University Press, Cambridge, 2003.

21. L. C. Cao, Y. L. Luo, S. H. Qiu, J. X. Liu, A perturbation method to the tent map based on Lyapunov exponent and its application, *Chin. Phys. B*, **24** (2015), 100501. https://doi.org/10.1088/1674-1056/24/10/100501

22. A. V. Korotayev, S. V. Tsirel, A spectral analysis of world GDP dynamics: Kondratieff waves, Kuznets swings, Juglar and Kitchin cycles in global economic development, and the 2008–2009 economic crisis, *Struct. Dyn.*, **4** (2010). https://doi.org/10.5070/SD941003306

23. P. Chen, A random walk or color chaos on the stock market? Time-frequency analysis of S & P indexes, *Stud. Nonlinear Dyn. Econom.*, **1** (1996). https://doi.org/10.2202/1558-3708.1014

24. J. B. Bassingthwaighte, L. S. Liebovitch, B. J. West, *Fractal Physiology*, Springer, New York, (2013).

25. T. Ai, R. Zhang, H. W. Zhou, J. L. Pei, Box-counting methods to directly estimate the fractal dimension of a rock surface, *Appl. Surf. Sci.*, **314** (2014), 610–621. https://doi.org/10.1016/j.apsusc.2014.06.152

26. Z. Q. Jiang, W. X. Zhou, D. Sornette, R. Woodard, K. Bastiaensen, P. Cauwels, Bubble diagnosis and prediction of the 2005–2007 and 2008–2009 Chinese stock market bubbles, *J. Econ. Behav. Organ.*, **74** (2010), 149–162. https://doi.org/10.1016/j.jebo.2010.02.007

27. D. Sornette, G. Demos, Q. Zhang, P. Cauwels, V. Filimonov, Q. Zhang, Real-time prediction and post-mortem analysis of the Shanghai 2015 stock market bubble and crash, in *Swiss Finance Institute Research Paper No. 15–31*, 2015. https://doi.org/10.2139/ssrn.2693634

28. E. C. Chang, J. W. Cheng, Y. Yu, Short-sales constraints and price discovery: evidence from the Hong Kong market, *J. Finance*, **62** (2007), 2097–2121. https://doi.org/10.1111/j.1540-6261.2007.01270.x

29. I. Yeung, N. Chiu, An outlier analysis of the Hong Kong stock market index, *Appl. Econ. Lett.*, **7** (2000), 531–534. https://doi.org/10.1080/13504850050033328

30. X. Gui, L. Li, J. Cao, L. Li, Dynamic communities in stock market, *Abstr. Appl. Anal.*, **2014** (2014), 723482. https://doi.org/10.1155/2014/723482

31. I. Khajar, The global stock exchange and its influence toward the indonesia stock exchange after the global financial crisis in 2008, *Int. J. Organ. Innovation*, **8** (2015), 133–154.

32. G. Zhang, J. Li, Multifractal analysis of Shanghai and Hong Kong stock markets before and after the connect program, *Physica A*, **503** (2018), 611–622. https://doi.org/10.1016/j.physa.2018.02.139

33. K. J. Lee, S. L. Lu, Y. Shih, Contagion effect of natural disaster and financial crisis events on international stock markets, *J. Risk Financ. Manag.*, **11** (2018), 16. https://doi.org/10.3390/jrfm11020016

34. T. Alexandra, Global woes hit stocks, *[EB/OL]*, 2022. Available from: https://money.cnn.com/2004/03/22/markets/markets_newyork/index.htm.

AIMS Press